Supporting Information

Screening Adsorbent-Water Adsorption Heat Pumps Based on Experimental Water Adsorption Isotherm Database

Zhilu Liu, [a,b] Wei Li, [a,b] Peyman Z. Moghadam [c] and Song Li [a,b,]*

[a] State Key Laboratory of Coal Combustion, School of Energy and Power Engineering, Huazhong University of Science and Technology, Wuhan 430074, China.

[b] Nano Interface Centre for Energy, School of Energy and Power Engineering, Huazhong University of Science and Technology, Wuhan 430074, China.

[c] Department of Chemical and Biological Engineering, The University of Sheffield, Mappin Street, Sheffield S1 3JD, UK

* Corresponding author email: songli@hust.edu.cn.

Table of Contents

Contents	Page Number

S1. Supplementary data

Table S1. Fitting parameters of water adsorption isotherms using universal adsorption isotherm model. (in Excel)

Table S2. Literatures for 232 adsorbents investigated in this work. (in Excel)

Table S3. Structural characteristics of adsorbents collected from literatures. (in Excel)

Table S4. The number of structural characteristics collected from literatures.

S_a (m^2/g)	No. of adsorbents	V_a (cm^3/g)	No. of adsorbents	D_p (Å)	No. of adsorbents
BET surface area	145	N_2 adsorption at 77 K	113	LCD	71
Langmuir surface area	3	Water adsorption at 298 K	6	Average pore diameter	46
		Mercury intrusion	4	Dominant pore size from PSD	19

Table S5. Adsorption characteristics and heat pump performances of adsorbent-water working pairs in adsorption cooling/heating system. (in Excel)

S2. Computation details based on the basic thermodynamic cycle of AHP
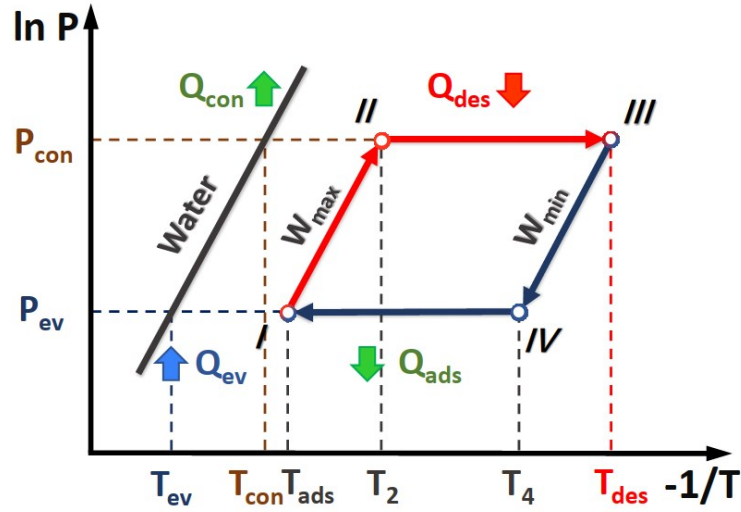
Figure S1. Basic thermodynamic cycle diagram of adsorption heat pump including isosteric heating (I-II), isobaric desorption (II-III), isosteric cooling (III-IV) and isobaric adsorption (IV-I).

As shown in the basic thermodynamic cycle diagram of AHP (Figure S1), T_{ev} and T_{con} are the temperature of evaporation and condensation, P_{ev} and P_{con} represent evaporation and condensation pressures, which equals the saturation pressure of water at T_{ev} and T_{con}, respectively. T_{ads} is adsorption temperature when adsorption process is completed, which equals T_{con} in this work. Similarly, T_{des} represents the temperature at end of desorption process. T_2 and T_4 are starting temperatures of adsorption and desorption in cycle, which can be obtained according to the generalized Trouton's rule[1] with fixed T_{ev}, T_{ads} and T_{des} ($T_2 = T_{con}^2/T_{ev}$ and $1/T_4 = 1/T_{des} - 1/T_2 + 1/T_{ads}$). Besides, the working capacity of water (ΔW) equals the difference of maximum water uptake (W_{max}) and minimum water uptake (W_{min}) (i.e. $W_{max} = W(T_{ads}, P_{ev})$ and $W_{min} = W(T_{des}, P_{con})$, $\Delta W = W_{max} - W_{min}$), both of which can be calculated by universal adsorption isotherm model (UAIM, Eq. 1).

Significantly, COP is defined as the useful energy output (SXE) divided by the energy input (Q_{input}). COP_C for cooling and COP_H for heating can be defined by the following equations, respectively.

$$COP_C = \frac{SCE}{Q_{input}} = \frac{Q_{ev}}{Q_{des}}$$

*

MERGEFORMAT (Eq. S1)

$$COP_H = \frac{SHE}{Q_{input}} = \frac{-(Q_{con} + Q_{ads})}{Q_{des}}$$

*

MERGEFORMAT (Eq. S2)

SCE is the specific cooling effects and SHE is the specific heating effects. SCE describing the energy transferred by working fluid for cooling equals the energy taken up in the evaporator (Q_{ev}), and Q_{input} is the heat energy from low-grade heat sources for desorption of adsorbent (Q_{des}). The useful energy output for heating is a combination of the energy released during condensation (Q_{con}) and the energy released during the adsorption stage (Q_{ads}). Both Q_{con} and Q_{ads} are negative values.

The relevant equations are listed below.

$$Q_{ev} = \Delta W \Delta_{vap} H(T_{ev}) + \Delta W \int_{T_{con}}^{T_{ev}} C_p^{wf}(T)\mathrm{d}T$$

*

MERGEFORMAT (Eq. S3)

$$Q_{con} = \Delta W \left[-\Delta_{vap} H(T_{con}) \right] + \Delta W \int_{T_{ev}}^{T_{con}} C_p^{wf}(T)\mathrm{d}T$$

*

MERGEFORMAT (Eq. S4)

$$\begin{aligned} Q_{des} &= Q_{I\text{-}II} + Q_{II\text{-}III} \\ &= \left[\int_{T_{ads}}^{T_2} C_p^{ad}(T)\mathrm{d}T + W_{max}\int_{T_{ads}}^{T_2} C_p^{wf}(T)\mathrm{d}T \right] + \left[\int_{T_2}^{T_{des}} C_p^{ad}(T)\mathrm{d}T + \int_{T_2}^{T_{des}} W(T)C_p^{wf}(T)\mathrm{d}T + \int_{W_{max}}^{W_{min}} \Delta_{ads}H(W)\mathrm{d}W \right] \end{aligned}$$

* MERGEFORMAT (Eq. S5)

$$\begin{aligned} Q_{ads} &= Q_{III\text{-}IV} + Q_{IV\text{-}I} \\ &= \left[\int_{T_{des}}^{T_4} C_p^{ad}(T)\mathrm{d}T + W_{min}\int_{T_{des}}^{T_4} C_p^{wf}(T)\mathrm{d}T \right] + \left[\int_{T_4}^{T_{ads}} C_p^{ad}(T)\mathrm{d}T + \int_{T_4}^{T_{ads}} W(T)C_p^{wf}(T)\mathrm{d}T + \int_{W_{min}}^{W_{max}} \Delta_{ads}H(W)\mathrm{dW} \right] \end{aligned}$$

* MERGEFORMAT (Eq. S6)

Here, for the regeneration process of adsorbents (i.e. steps of I-II and II-III), $\int_{T_{ads}}^{T_2} C_p^{ad}(T)dT$

and $\int_{T_2}^{T_{des}} C_p^{ad}(T)dT$ are the energy required for the adsorbent bed temperature to change from

T_{ads} to T_{des}, in which only adsorbents were taken into account. $\int_{W_{max}}^{W_{min}} \Delta_{ads}H(W)dW$ is the heat

adsorbed for water desorption in the AHP system. A similar analysis was performed for the energy transfer during adsorption stage (Q_{ads}). In these formulas, the specific heat capacity

(C_p) of the adsorbent (C_p^{ad})and water working fluid (C_p^{wf}) are 1 kJ/(kg·K) (reasonable value

for a variety of adsorbents)[2] and 4.2 kJ/(kg·K), respectively.

The specific heat capacity of the adsorbent (C_p^{ad}) is a constant value of 1.0 J/(g·K) according

to the variation of heat capacity of typical adsorbents shown in Table S5. Such slight

variation in C_p^{ad} of adsorbents will not impose significant impacts on COP_C as demonstrated

in Figure S2.

Additionally, the vaporization enthalpy ($\Delta_{vap}H$ in kJ/kg) of water is a function of temperature.

$$\Delta_{vap}H(T) = -2.51(T - 273) + 2502 \qquad \backslash *$$

MERGEFORMAT (Eq. S7)

The enthalpy of adsorption ($\Delta_{ads}H$) is calculated using the predicted adsorption isotherms obtained by the universal isotherm adsorption model at varying temperatures according to the Clausius-Clapeyron equation shown in Eq. S8.

$$\Delta_{ads}H = -R\frac{\partial(\ln p)}{\partial(1/T)} \qquad \backslash *$$

MERGEFORMAT (Eq. S8)

Then, the formula for calculating COP can be obtained by substitution and simplification.

$$SCE = \Delta W\left[\Delta_{vap}H(T_{ev}) - C_p^{wf}(T_{con} - T_{ev})\right] \qquad \backslash *$$

MERGEFORMAT (Eq. S9)

$$\text{COP}_{\text{C}} = \frac{\Delta W \left[\Delta_{\text{vap}} H \left(T_{\text{ev}} \right) - C_{\text{p}}^{\text{wf}} \left(T_{\text{con}} - T_{\text{ev}} \right) \right]}{C_{\text{p}}^{\text{ad}} \left(T_{\text{des}} - T_{\text{ads}} \right) + C_{\text{p}}^{\text{wf}} \left[W_{\text{max}} \left(T_2 - T_{\text{ads}} \right) + \int_{T_2}^{T_{\text{des}}} W(T) \mathrm{d}T \right] - \Delta W \Delta_{\text{ads}} H}$$
*

MERGEFORMAT (Eq. S10)

$$\text{SHE} = \Delta W \left[\Delta_{\text{vap}} H \left(T_{\text{con}} \right) - C_{\text{p}}^{\text{wf}} \left(T_{\text{con}} - T_{\text{ev}} \right) - \Delta_{\text{ads}} H \right] + C_{\text{p}}^{\text{ad}} \left(T_{\text{des}} - T_{\text{ads}} \right) + C_{\text{p}}^{\text{wf}} \left[W_{\text{min}} \left(T_{\text{des}} - T_4 \right) + \int_{T_{\text{ads}}}^{T_4} W(T) \mathrm{d}T \right]$$

* MERGEFORMAT (Eq. S11)

$$\text{COP}_{\text{H}} = \frac{\Delta W \left[\Delta_{\text{vap}} H \left(T_{\text{con}} \right) - C_{\text{p}}^{\text{wf}} \left(T_{\text{con}} - T_{\text{ev}} \right) - \Delta_{\text{ads}} H \right] + C_{\text{p}}^{\text{ad}} \left(T_{\text{des}} - T_{\text{ads}} \right) + C_{\text{p}}^{\text{wf}} \left[W_{\text{min}} \left(T_{\text{des}} - T_4 \right) + \int_{T_{\text{ads}}}^{T_4} W(T) \mathrm{d}T \right]}{C_{\text{p}}^{\text{ad}} \left(T_{\text{des}} - T_{\text{ads}} \right) + C_{\text{p}}^{\text{wf}} \left[W_{\text{max}} \left(T_2 - T_{\text{ads}} \right) + \int_{T_2}^{T_{\text{des}}} W(T) \mathrm{d}T \right] - \Delta W \Delta_{\text{ads}} H}$$

* MERGEFORMAT (Eq. S12)

Table S5. Specific heat capacity of typical MOFs, carbon, zeolites and silicic adsorbents.

Species	Adsorbents	Heat of capacity (J/(g·K))
MOFs	Cu-BTC	0.78-0.88 (333 K-423 K) [3]
	MOF-177	0.82-0.99 (333 K-423 K) [3]
Carbon	AC Maxsorb III	0.84-1.07 (303 K-423 K) [4]
	EC-1500	0.74-1.03 (303 K-423 K) [4]
Zeolites	Zeolite 4A	0.86-0.95 (272 K-311 K) [5]
	Zeolite NaX	0.81-0.84 (283 K-303 K) [6]
Silicic Materials	Silica Gel RD type	0.87-1.01 (303 K-373 K) [7]
	Silica Gel type A	0.89-1.03 (303 K-373 K) [7]
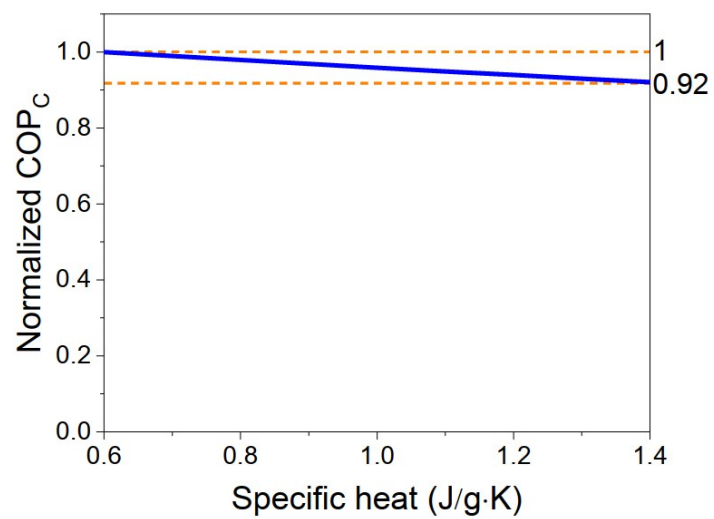
Figure S2. Normalized COP_C as a function of specific heat capacity.

S3. Structure-performance relationships of adsorbent-water working pairs.

Table S6. The number and percentage of adsorbents sorted by COP_C under cooling conditions.

Rank	Number and percentage					
	MOFs	Carbon	Zeolites	Silicic Materials	Composites	Others
Top 10	10 (100%)	0	0	0	0	0
Top 30	27 (90%)	0	1 (3.33%)	2 (6.67%)	0	0
Top 50	45 (90%)	2 (4%)	1 (2%)	2 (4%)	0	0
Top 100	88 (88%)	5 (5%)	5 (5%)	2 (4%)	0	0
Sum 231	163 (70.56%)	36 (15.58%)	10 (4.33%)	11 (4.76%)	7 (3.03%)	4 (1.73%)

Table S7. The number and percentage of adsorbents sorted by COP_H under heating conditions.

Rank	Number and percentage					
	MOFs	Carbon	Zeolites	Silicic Materials	Composites	Others
Top 10	10 (100%)	0	0	0	0	0
Top 30	27 (90%)	0	3 (10%)	0	0	0
Top 50	43 (86%)	0	5 (10%)	2 (4%)	0	0
Top 100	84 (84 %)	5 (5%)	7 (7%)	3 (3%)	0	1 (1%)
Sum 231	163 (70.56%)	36 (15.58%)	10 (4.33%)	11 (4.76%)	7 (3.03%)	4 (1.73%)

Table S8. Comparison of the predicted COP of high-performing adsorbents in this work with previous studies.

Working conditions	Adsorbents	COP in this work	Reported COP	Same adsorption isotherms?
Cooling	Zr-MOF-841	0.839	0.82 [2]	Yes
	DUT-67	0.793	0.78 [8]	No
	MIL-125-NH$_2$	0.792	0.77-0.8 [9]	No
	UiO-66(Zr^{4+}) with high concentration stearic acid	0.768	0.60 [10]	No
	Cr-MIL(101)	0.759	0.57 [11]	No
Heating	MIL-160	1.673	1.65 [12]	Yes
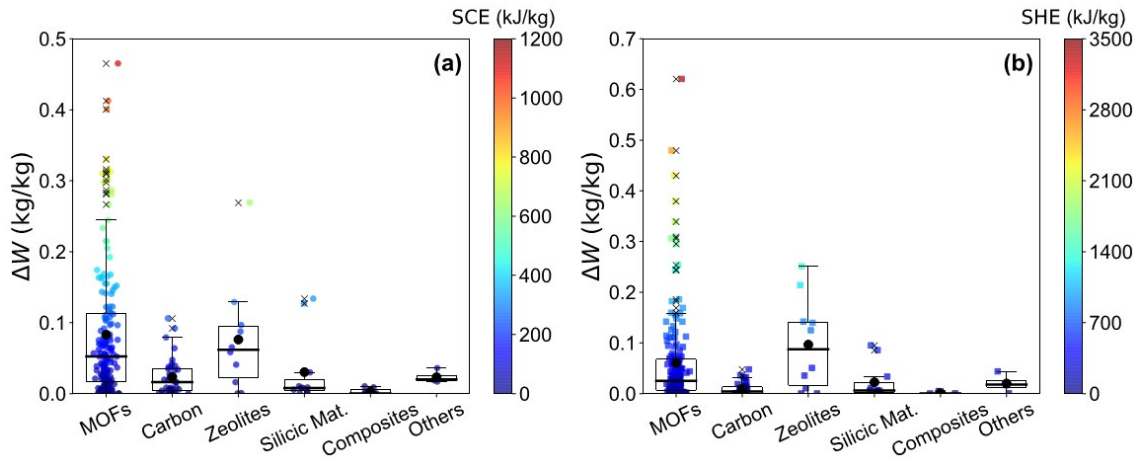
Figure S3. The distribution of different adsorbent species exhibiting different water working capacities (ΔW) and the specific effects (SXE) for (a) adsorption cooling and (b) heating. The operational conditions are fixed at P_{ev} =1221 Pa, P_{con} =4231 Pa, T_{ev} =283 K, T_{con} = T_{ads} = 303 K, T_{des} = 368 K for cooling and P_{ev} =1697 Pa, P_{con} = 9559 Pa, T_{ev} =288 K, T_{con} = T_{ads} =318 K, T_{des} = 413 K for heating.

Table S9. The number of adsorbents exhibiting different step positions (α).

α	Adsorbent species	Number

	MOFs	Carbon	Zeolites	Silicic materials	Composites	Others	
0.0-0.1	55	3	8	6	–	3	75
0.1-0.2	19	–	–	1	–	–	20
0.2-0.3	15	5	–	–	–	–	20
0.3-0.4	17	2	–	1	–	–	20
0.4-0.5	13	4	–	–	2	–	19
0.5-0.6	6	5	–	–	2	–	13
0.6-0.7	5	7	–	–	1	–	13
0.7-0.8	10	1	1	1	–	–	13
0.8-0.9	8	2	1	2	2	1	16
0.9-1.0	15	7	–	–	–	–	22
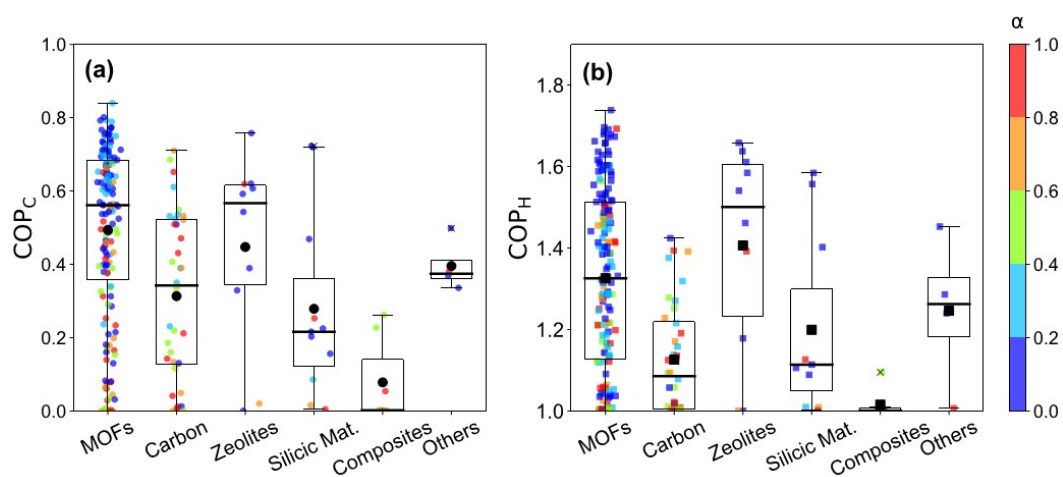
Figure S4. The distribution of different adsorbents exhibiting varying coefficient of performance (COP) and the step position (α) of adsorption isotherms for (a) adsorption cooling and (b) heating. COP_C and COP_H were both obtained at fixed operational temperatures, COP_C was obtained at T_{ev} =283 K, $T_{con} = T_{ads} = 303$ K, $T_{des} = 368$ K, and COP_H was calculated at T_{ev} =288 K, $T_{con} = T_{ads}$ =318 K, $T_{des} = 413$ K.
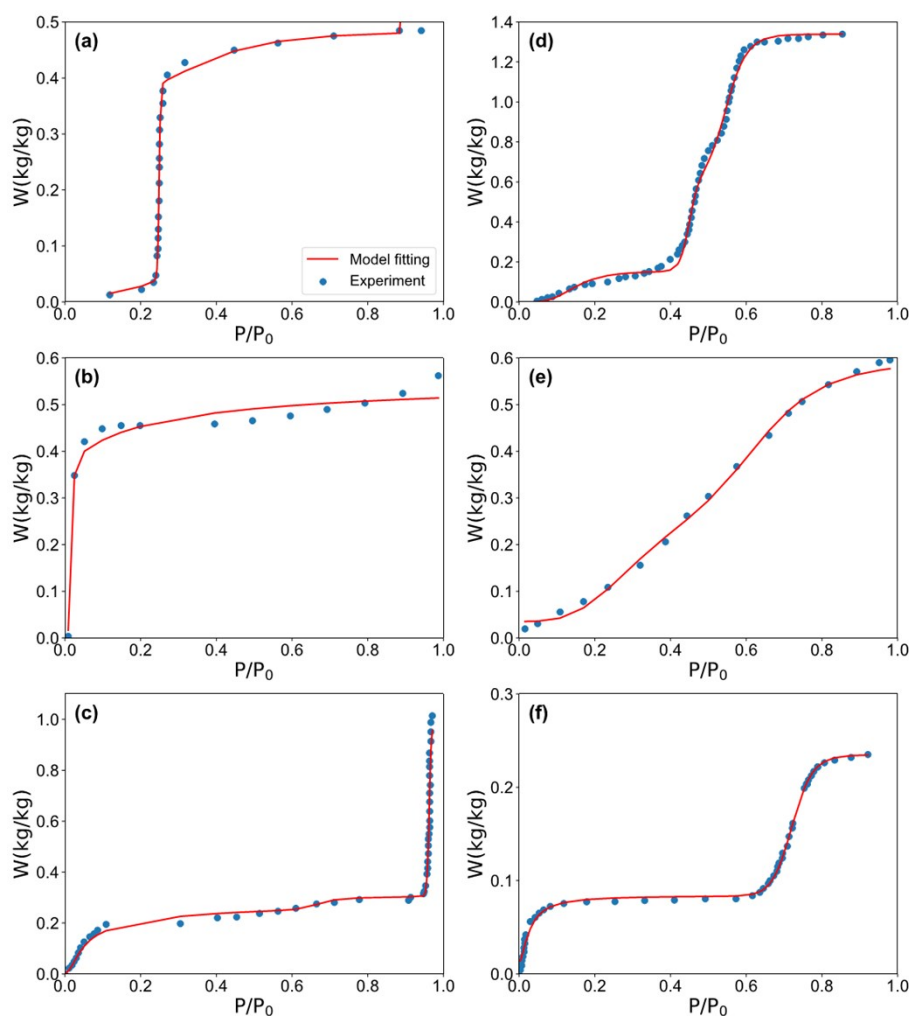
Figure S5. The experimental water adsorption isotherms fitted by using universal adsorption isotherm model. (a) Zr-MOF-841[13], (b) Ni-DOBDC[14], (c) HKUST-1-F[15], (d) Cr-MIL(101)[16], (e) Activated Carbon AT800R15t120[17], (f) (H$_2$dab)[Zn$_2$(ox)$_3$][18].

Table S10. The number of adsorbents with different structural properties provided in literatures.

Structural characteristics	Adsorbent species						Number
	MOFs	Carbon	Zeolite	Silicic Material	Composite	Others	
S_a [a]	95	31	6	6	6	4	148
V_a [b]	69	33	6	6	6	3	123
D_p [c]	104	17	7	3	3	2	136

[a] S_a of 147 adsorbents is the Brunauer-Emmett-Teller (BET) surface area and 3 adsorbents used Langmuir surface area.

[b] V_a of most adsorbents (115 adsorbents) are obtained from N_2 adsorption isotherms at 77K, while V_a of 6 adsorbents were obtained from water adsorption isotherms at 298 K, and the rest was measured by using mercury intrusion method.

[c] D_p was defined in three different ways according to literature, including the average pore diameter prioritized for 46 adsorbents, the largest cavity diameter (LCD) when multiple pores sizes were provided in literature for 71 adsorbents, and the dominant pore size if only the pore size distribution (PSD) were provided for 19 adsorbents.

References

1. Aristov, Y. I.; Tokarev, M. M.; Sharonov, V. E., Universal relation between the boundary temperatures of a basic cycle of sorption heat machines. *Chem. Eng. Sci.* **2008,** *63* (11), 2907-2912.

2. de Lange, M. F.; Verouden, K. J.; Vlugt, T. J.; Gascon, J.; Kapteijn, F., Adsorption-Driven Heat Pumps: The Potential of Metal-Organic Frameworks. *Chem. Rev.* **2015,** *115* (22), 12205-50.

3. Mu, B.; Walton, K. S., Thermal Analysis and Heat Capacity Study of Metal–Organic Frameworks. *J. Phys. Chem. C* **2011,** *115* (46), 22748-22754.

4. Uddin, K.; Amirul Islam, M.; Mitra, S.; Lee, J.-b.; Thu, K.; Saha, B. B.; Koyama, S., Specific heat capacities of carbon-based adsorbents for adsorption heat pump application. *Appl. Therm. Eng.* **2018,** *129*, 117-126.

5. Qiu, L. Y.; Murashov, V.; White, M. A., Zeolite 4A: heat capacity and thermodynamic properties. *Solid State Sciences* **2000,** *2* (8), 841-846.

6. Qiu, L.; Laws, P. A.; Zhan, B.-Z.; White, M. A., Thermodynamic investigations of zeolites NaX and NaY. *Can. J. Chem.* **2006,** *84* (2), 134-139.

7. Islam, M. A.; Pal, A.; Saha, B. B., Experimental study on thermophysical and porous properties of silica gels. *Int. J. Refrig.* **2020,** *110*, 277-285.

8. Bon, V.; Senkovska, I.; Evans, J. D.; Wöllner, M.; Hölzel, M.; Kaskel, S., Insights into the water adsorption mechanism in the chemically stable zirconium-based MOF DUT-67–a prospective material for adsorption-driven heat transformations. *J. Mater. Chem. A* **2019,** *7* (20), 12681-12690.

9. Gordeeva, L. G.; Solovyeva, M. V.; Aristov, Y. I., NH2-MIL-125 as a promising material for adsorptive heat transformation and storage. *Energy* **2016,** *100*, 18-24.

10. Xia, X.; Cao, M.; Liu, Z.; Li, W.; Li, S., Elucidation of adsorption cooling characteristics of Zr-MOFs: Effects of structure property and working fluids. *Chem. Eng. Sci.* **2019,** *204*, 48-58.

11. Graf, S.; Redder, F.; Bau, U.; de Lange, M.; Kapteijn, F.; Bardow, A., Toward Optimal Metal–Organic Frameworks for Adsorption Chillers: Insights from the Scale-Up of MIL-101(Cr) and NH2-MIL-125. *Energy Technology* **2019,** *8* (1), 1900617.

12. Cadiau, A.; Lee, J. S.; Damasceno Borges, D.; Fabry, P.; Devic, T.; Wharmby, M. T.; Martineau, C.; Foucher, D.; Taulelle, F.; Jun, C. H.; Hwang, Y. K.; Stock, N.; De Lange, M. F.;

Kapteijn, F.; Gascon, J.; Maurin, G.; Chang, J. S.; Serre, C., Design of hydrophilic metal organic framework water adsorbents for heat reallocation. *Adv. Mater.* **2015,** *27* (32), 4775-80.

13. Furukawa, H.; Gandara, F.; Zhang, Y. B.; Jiang, J.; Queen, W. L.; Hudson, M. R.; Yaghi, O. M., Water adsorption in porous metal-organic frameworks and related materials. *J. Am. Chem. Soc.* **2014,** *136* (11), 4369-4381.

14. Liu, J.; Wang, Y.; Benin, A. I.; Jakubczak, P.; Willis, R. R.; LeVan, M. D., CO2/H2O adsorption equilibrium and rates on metal-organic frameworks: HKUST-1 and Ni/DOBDC. *Langmuir* **2010,** *26* (17), 14301-7.

15. Ko, N.; Hong, J.; You, L.; Park, H. J.; Yang, J. K.; Kim, J., Chemical Property Change in a Metal-Organic Framework by Fluoro Functionality. *Bull. Korean Chem. Soc.* **2015,** *36* (1), 327-332.

16. Canivet, J.; Fateeva, A.; Guo, Y.; Coasne, B.; Farrusseng, D., Water adsorption in MOFs: fundamentals and applications. *Chem. Soc. Rev.* **2014,** *43* (16), 5594-617.

17. Martínez de Yuso, A.; Izquierdo, M. T.; Rubio, B.; Carrott, P. J. M., Adsorption of toluene and toluene–water vapor mixture on almond shell based activated carbons. *Adsorption* **2013,** *19* (6), 1137-1148.

18. Sadakiyo, M.; Yamada, T.; Kitagawa, H., Hydroxyl group recognition by hydrogen-bonding donor and acceptor sites embedded in a layered metal-organic framework. *J. Am. Chem. Soc.* **2011,** *133* (29), 11050-3.